COHERENCE FILTERING TO ENHANCE THE MANDIBULAR CANAL IN CONE-BEAM CT DATA

D. Kroon[1], C.H. Slump[1]

[1]Signals and Systems, University of Twente, Netherlands

Abstract

Segmenting the mandibular canal from cone beam CT data, is difficult due to low edge contrast and high image noise. We introduce 3D coherence filtering as a method to close the interrupted edges and denoise the structure of the mandibular canal. Coherence Filtering is an anisotropic non-linear tensor based diffusion algorithm for edge enhancing image filtering. We test different numerical schemes of the tensor diffusion equation, non-negative, standard discretization and also a rotation invariant scheme of Weickert [1]. Only the scheme of Weickert did not blur the high spherical images frequencies on the image diagonals of our test volume. Thus this scheme is chosen to enhance the small curved mandibular canal structure. The best choice of the diffusion equation parameters c_1 and c_2, depends on the image noise. Coherence filtering on the CBCT-scan works well, the noise in the mandibular canal is gone and the edges are connected. Because the algorithm is tensor based it cannot deal with edge joints or splits, thus is less fit for more complex image structures.

1 Introduction

Accurate information about the location of the mandibular canal is essential in case of dental surgery [2], because violation of the canal space during implant placement can damage the inferior alveolar nerve or blood vessels. Cone beam CT (CBCT) is becoming an increasingly utilized imaging modality in dental examinations, with a factor of ten lower dose than conventional CT [3]. We tested automatic canal segmentation methods from literature such as the Fast Marching Method on CBCT scans. These methods fail on CBCT scans because of higher noise, missing ridges and less contrast between mandibular canal and surrounding tissue than in conventional CT.

In this research we focus on improving the CBCT image quality by filtering the data to remove noise and enhance the edges, with smoothing which adapts to the underlying image structure to preserve edges.

We introduce 3D nonlinear anisotropic diffusion filtering which is based on the 2D coherence enhancing diffusion introduced by Weickert. The diffusion tensor in this method is oriented using an image structure tensor, with a kernel which is elongated in the direction of the underlying image edges. There are many possible ways to discretize the continuous diffusion tensor equations and image derivatives. We will evaluate the influence of several discretization schemes and parameters choices.

2 Coherence Filtering

The anisotropic diffusion filtering method consist of two steps. The first is describing the image structure with the commonly used structure tensor also referred to as the "second-moment matrix". The second step is transforming the structure tensor into a diffusion tensor for edge enhancing diffusion filtering.

2.1 Step 1, Structure Tensor

Let $I(\mathbf{x})$ denote a 3D image, where $\mathbf{x} = (x, y, z)$ is the coordinate vector. The structure tensor of a coordinate in the image I is a symmetric positive semi-definite 3×3 tensor given by

$$\mathbf{J}\left(\nabla I\right) = K_j * \left(\nabla I \cdot \nabla I^T\right) \quad (1)$$

With ∇I the image gradient, and K_j a Gaussian weighting function with sigma ρ. The eigen-analysis of this structure tensor will give the orientation of the local image features:

$$\mathbf{J}\left(\nabla I\right) = [\mathbf{v_1}\mathbf{v_2}\mathbf{v_3}] \cdot \begin{bmatrix} \mu_1 & 0 & 0 \\ 0 & \mu_2 & 0 \\ 0 & 0 & \mu_3 \end{bmatrix} \cdot \begin{bmatrix} \mathbf{v_1}^T \\ \mathbf{v_2}^T \\ \mathbf{v_3}^T \end{bmatrix} \quad (2)$$

The eigen vectors $\mathbf{v_1}, \mathbf{v_2}, \mathbf{v_3}$ give the local image orientations, with $\mathbf{v_1} = [v_{11}, v_{12}, v_{13}]^T$. With eigen values $\mu_1 \geq \mu_2 \geq \mu_3$ describing the average contrast in those directions.

2.2 Step 2, Diffusion Tensor

The diffusion tensor filtering equation is described by:

$$\frac{\delta u}{\delta t} = \nabla \cdot (\mathbf{D}\nabla u) \tag{3}$$

The natural way is to use the same eigenvector orientations for the diffusion tensor $\mathbf{D}$ as given by the structure tensor:

$$\mathbf{D} = \begin{bmatrix} D_{11} & D_{12} & D_{13} \\ D_{12} & D_{22} & D_{23} \\ D_{13} & D_{23} & D_{33} \end{bmatrix} \tag{4}$$

$$
\begin{aligned}
D_{11} &= \lambda_1 v_{11}^2 + \lambda_2 v_{21}^2 + \lambda_3 v_{31}^2 \\
D_{22} &= \lambda_1 v_{12}^2 + \lambda_2 v_{22}^2 + \lambda_3 v_{32}^2 \\
D_{33} &= \lambda_1 v_{13}^2 + \lambda_2 v_{23}^2 + \lambda_3 v_{33}^2 \\
D_{12} &= \lambda_1 v_{11}v_{12} + \lambda_2 v_{21}v_{22} + \lambda_3 v_{31}v_{32} \\
D_{13} &= \lambda_1 v_{11}v_{13} + \lambda_2 v_{21}v_{23} + \lambda_3 v_{31}v_{33} \\
D_{23} &= \lambda_1 v_{12}v_{13} + \lambda_2 v_{22}v_{23} + \lambda_3 v_{32}v_{33}
\end{aligned} \tag{5}
$$

The eigenvalues $\lambda_1, \lambda_2, \lambda_3$ are calculated with a from 2D to 3D extended equation of Weickert [1]. There are other edge enhancing eigenvalue equations in literature, but they often require edge threshold values [4]. Extension from 2D to 3D gives two possibilities, line enhancement [5]

$$
\begin{aligned}
\lambda_1 &: = c_1 \\
\lambda_2 &: = c_1 \\
\lambda_3 &: = c_1 + (1 - c_1)\exp\left(\frac{-c_2}{(\mu_1 - \mu_3)^2}\right)
\end{aligned} \tag{6}
$$

or plane enhancement

$$
\begin{aligned}
\lambda_1 &:= c_1 \\
\lambda_2 &:= c_1 + (1 - c_1)\exp\left(\frac{-c_2}{(\mu_2 - \mu_3)^2}\right) \\
\lambda_3 &:= c_1 + (1 - c_1)\exp\left(\frac{-c_2}{(\mu_1 - \mu_3)^2}\right)
\end{aligned} \tag{7}
$$

with $c_1 \in (0, 1)$ a global smoothing constant, and $c_2 > 0$ the edge enhancing smoothing constant.

The described edge enhancing diffusion filtering is repeated in an iterative way. The number of iterations is set by the user, and will determine the amount of smoothing.

3 Known Limitations

The described method to find the image structure orientations is comparable to the vesselness filter of Frangi et al. [6]. Using the structure tensor to find the orientations is more robust against noise than the Hessian used by Frangi, but a combination of both methods gives the best cylindrical structure detection [7] . We will only use the structure tensor because second order derivatives of a 3D volume are CPU expensive. Frangi uses a Gaussian scale space to find vessels of different sizes, diffusion filtering only uses one scale thus does not perform equally on lines of different widths. There is one principle limitation of tensors, they cannot model complex image structures only symmetric spherical shapes. This causes vesselness filtering like Frangi to fail on vessel joints and Diffusion Tensor imaging (DTI) on touching and splitting nerves. A possible solution is describing each image coordinate with multiple tensors.

4 Numerical Discretization

The image I is a discrete function thus the equations must be discretized. First we describe derivate discretization, secondly different diffusion schemes, and at last a rotation invariance diffusion scheme.

4.1 Derivatives

The gradient ∇I can be implement with several numeric methods. Most commonly the image is low pass filtered with a Gaussian kernel K_i with sigma σ followed by central differences. Instead of central differences also the truncated derivatives of a Gaussian kernel or Sobel kernel can be used. Scharr et al. changed the smoothing values $[1, 2, 1]$ of the commonly used Sobel kernel to $[3, 10, 3]$, which give more rotation invariant derivatives.

4.2 Diffusion Schemes

The tensor diffusion equation 3 can be solved numerically using finite differences. The common way is to replace spatial differences with central differences [5] and use for $\frac{\delta u}{\delta t}$ a forward difference approximation [1]:

$$
\begin{aligned}
\frac{u_{i,j}^{k+1} - u_{i,j}^k}{\tau} &= A_{i,j}^k * u_{i,j}^k \Rightarrow \\
u_{i,j}^{k+1} &= \left(I + \tau A_{i,j}^k\right) * u_{i,j}^k
\end{aligned} \tag{8}
$$

Where τ is the time step size and $u_{i,j}^k$ denotes the approximation of $u(x, t)$ in pixel (i, j) at time $k\tau$. The expression $A_{i,j}^k * u_{i,j}^k$ is a discretization of $\nabla \cdot (\mathbf{D}\nabla u)$. Thus convolution with a spatially and temporally varying mask $A_{i,j}^k$ also called stencil gives the diffusion update. Two common discretizations are the so-called standard discretization [8] and non-negative discretization using a $3 \times 3 \times 3$ stencil. Stability is an issue with

these schemes, and only a small time step is allowed $\tau \leq 0.5/n$, with n the number of image dimensions. To allow large time steps implicit discretization schemes were introduced, and explicit schemes stabilized by means of additive operator splitting (AOS).

4.3 Rotation Invariant Scheme

Rotation invariant anisotropic diffusion is important with curved like structures such as the mandibular canal. Weickert showed that larger stencils than 3×3 in 2D are needed to fix the number of degrees of freedom of the kernel to allow rotation invariance; so he introduced a 5×5 stencil. We can write the divergence operator equation 3 in 3D as:

$$\nabla \cdot (\mathbf{D}\nabla u) = \partial_x j_1 + \partial_y j_2 + \partial_z j_3 \qquad (9)$$

With j_1, j_2, j_3 the flux components which are described by:

$$
\begin{aligned}
j_1 &:= D_{11}\left(\partial_x u\right) + D_{12}\left(\partial_y u\right) + D_{13}\left(\partial_z u\right) \\
j_2 &:= D_{12}\left(\partial_x u\right) + D_{22}\left(\partial_y u\right) + D_{23}\left(\partial_z u\right) \quad (10) \\
j_3 &:= D_{13}\left(\partial_x u\right) + D_{23}\left(\partial_y u\right) + D_{33}\left(\partial_z u\right)
\end{aligned}
$$

The image derivatives such as $\partial_x u$ are calculated by using the Sobel filter with values of Scharr, the same kernel is used to calculated the derivatives of the flux components. There is no need to combine above equations into a real $5 \times 5 \times 5$ stencil, because that will result in more calculations for the same result.

5 Results

We perform three tests. The first to find the most suitable diffusion scheme, the second to test the influence of the involved parameters. The last test is filtering a CBCT scan, to evaluate the performance on the mandibular canal.

5.1 Scheme Comparison

First, we compare the performance of the 3D diffusion schemes: the standard, non-negative and the $5 \times 5 \times 5$ scheme of Weickert. We use a spherical image with varying frequencies to test rotational performance, also uniform noise is added to measure filtering performance. We use a diffusion time of $15s$ and small time step of $0.1s$, the diffusion parameters are chosen : $c_1 = 0.001$, $c_2 = 10^{-10}$, $\rho = 1$, $\sigma = 1$.

The standard and non-negative schemes show large blurring artifacts on image diagonals especially at the finer structures, figure 1. The most suitable scheme for the curved mandibular canal is the $5 \times 5 \times 5$ line filtering
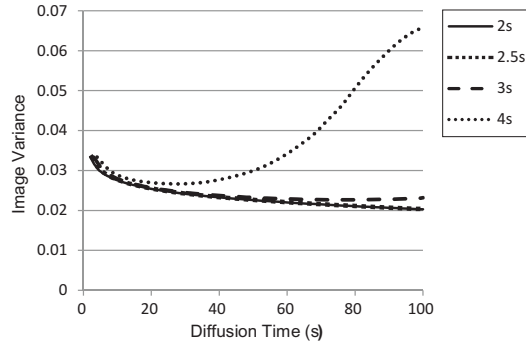
Figure 2: Stability test of $5 \times 5 \times 5$ scheme

scheme, despite of small checkerboard artifacts. The time needed to perform 150 iterations on this $257 \times 257 \times 257$ volume with a Intel Core 2 Duo is in the order of 30 minutes for all schemes.

5.2 Parameters

A constant decreasing image variance is one of the main principles of iterative noise filtering. By looking at the image variance while filtering with a number of diffusion step sizes we will find the maximum time step for which our $5 \times 5 \times 5$ stencil is stable, figure 2. The maximum stable step size found is $2.5s$, with a higher value small regions with very high and very low values start to occur.

We also test the influence of c_1 on the filtering of the spherical frequencies volume. Setting the constant to 10^{-3} gives the smallest squared difference between test and noise filtered volume. Setting the constant higher results in Gaussian smoothing. If you set c_1 to low for instance 10^{-8}, it will causes more severe chessboard artifacts, and uniform areas are less denoised.

The second constant c_2 determines if the diffusion behaves like an edge enhancing diffusion (EED) [5] or coherence enhancing diffusion (CED). CED will close interrupted lines and flow-like structures, by steering the diffusion flux to the outbalanced direction. Coherence enhancing diffusion is less robust against noise, will not blur uniform regions (because there $\mu_1 = \mu_3$), and will smear out endpoints of image lines. Setting the c_2 constant to 10^{-10} which effectively is EED filtering, gives the smallest squared difference between filtered and spherical test volume. The denominator term of Weickerts equation, $mu_1 - mu_3$ will depend on the relation between structure and noise. Thus the value of c_2 should be chosen by the user depending on amount of noise in the image and the need for edge enhancement.
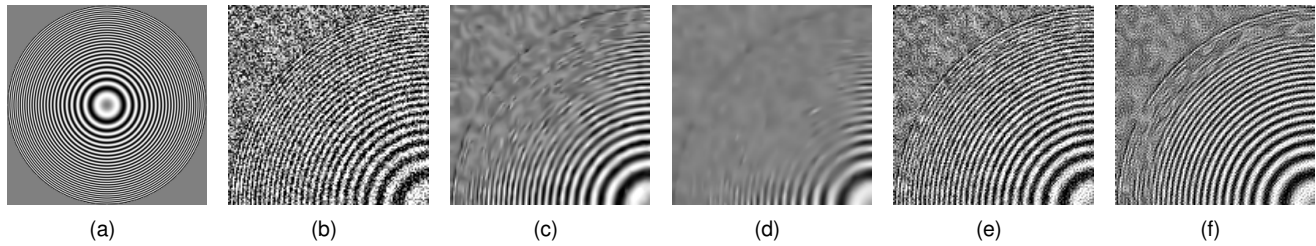
Figure 1: Performance of different 3D diffusion schemes. (a) Spherical Frequencies, (b) Uniform Noise added, (c) Standard, (d) Non-negative, (e) $5 \times 5 \times 5$ line filtering, (f) $5 \times 5 \times 5$ surface filtering
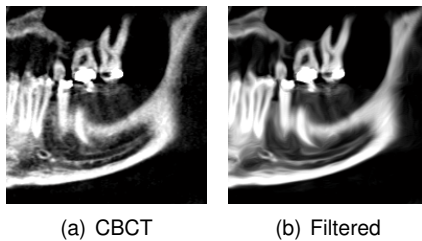

(a) CBCT   (b) Filtered

Figure 3: Mandibular CBCT scan, coherence filtered with $5 \times 5 \times 5$ stencil, and after filtering geometrically transformed to a dental scan like volume. Part of a slice with channel is shown here.

5.3 Mandibular Canal

We filtered a cone beam CT dataset of the head of a dental patient with dimensions $400 \times 400 \times 552$ and a uniform voxel resolution of 0.4mm. We used the $5 \times 5 \times 5$ scheme with coherence filtering parameters: time step $2s$ total diffusion time $10s$, $c_2 = 10-5$, $c_1 = 10-3$, $\sigma = 1$ and $\rho = 2$. An image of the filtering result is shown in figure 3. The noise in the channel has disappeared and the edges are enhanced and connected. The CPU-time needed was 459 seconds, which could eventually be improved by explicitly using SSE instructions.

6 Conclusions

The tensor model cannot model edge joints or splits, which makes it unsuitable for complex image structures. The best discretization scheme for small curved edges and ridges is the $5 \times 5 \times 5$ diffusion scheme of Weickert. Main disadvantage of this scheme are chessboard like artifacts due to central differences, also noise is preserved in uniform image regions. Coherence filtering of a CBCT scan took 8 minutes, and successfully enhanced the edges of the mandibular canal. Main conclusion, coherence filtering with a $5 \times 5 \times 5$ stencil is suitable as pre-processing for automatically mandibular canal segmentation.

7 References

[1] Weickert J, Scharr H. A scheme for coherence-enhancing diffusion filtering with optimized rotation invariance. Journal of Visual Communication and Image Representation 2002;13(1):103–118.

[2] Dario L. Implant placement above a bifurcated mandibular canal: a case report. Implant Dentistry 2002; 11(3):258–256.

[3] Roberts J, Drage N, Davies. J, Thomas D. Effective dose from cone beam CT examinations in dentistry. The British Journal of Radiology 2009;82:35–40.

[4] Tabik S, Garzn E, Garca I, Fernndez J. Multiprocessing of anisotropic nonlinear diffusion for filtering 3d images. 2006; 21–27.

[5] Frangakis A, Hegerl R. Noise reduction in electron tomographic reconstructions using nonlinear anisotropic diffusion. Journal of Structural Biology 2001;(135):239–250.

[6] Frangi A, Frangi R, Niessen W, Vincken K, Viergever M. Multiscale vessel enhancement filtering. Springer-Verlag, 1998; 130–137.

[7] Good W, Wang X, Fuhrman C, Sumkin J, Maitz G, Leader J, Britton C, Gur D. Application of 3D geometric tensors for segmenting cylindrical tree structures from volumetric datasets. In SPIE Conference Series, volume 6512. 2007; .

[8] Fritz L. Diffusion-based applications for interactive medical image segmentation. In Proceedings of CESCG 2006. 2006; .